J Mater Sci: Mater Med (2013) 24:2037–2046
DOI 10.1007/s10856-013-4944-z

A silk fibroin/chitosan scaffold in combination with bone marrow-derived mesenchymal stem cells to repair cartilage defects in the rabbit knee

Jiang Deng · Rongfeng She · Wenliang Huang · Zhijun Dong · Gang Mo · Bin Liu

Received: 5 September 2012 / Accepted: 29 April 2013 / Published online: 16 May 2013

Abstract Bone marrow-derived mesenchymal stem cells (BMSCs) were seeded in a three-dimensional scaffold of silk fibroin (SF) and chitosan (CS) to repair cartilage defects in the rabbit knee. Totally 54 rabbits were randomly assigned to BMSCs + SF/CS scaffold, SF/CS scaffold and control groups. A cylindrical defect was created at the patellofemoral facet of the right knee of each rabbit and repaired by scaffold respectively. Samples were prepared at 4, 8 and 12 weeks post-surgery for gross observation, hematoxylin–eosin and toluidine blue staining, type II collagen immunohistochemistry, Wakitani histology. The results showed that differentiated BMSCs proliferated well in the scaffold. In the BMSCs + SF/CS scaffold group, the bone defect was nearly repaired, the scaffold was absorbed and immunohistochemistry was positive. In the SF/CS scaffold alone group, fiber-like tissues were observed, the scaffold was nearly degraded and immunohistochemistry was weakly positive. In the control group, the defect was not well repaired and positive immunoreactions were not detected. Modified Wakitani scores were superior in the BMSCs + SF/CS scaffold group compared with those in other groups at 4, 8 and 12 weeks ($P < 0.05$). A SF/CS scaffold can serve as carrier for stem cells to repair cartilage defects and may be used for cartilage tissue engineering.

J. Deng (✉) · W. Huang · Z. Dong · G. Mo · B. Liu
Department of Orthopedics, Third Affiliated Hospital of Zunyi Medical College, 98 Fenghuang Road, Zunyi 563002, Guizhou Province, China
e-mail: jiangdeng2011@163.com

R. She
Department of Orthodontics, Guizhou Provincial People's Hospital, 83 East Zhongshan Road, Guiyang 550002, Guizhou Province, China

1 Introduction

Joint degeneration is progressive with aging. In the elderly, joint degeneration results in joint dysfunction. The self-repair of adult cartilage tissues is poor [1]. Therefore, inadequate repair of cartilage defects has provoked increasing concern. Autologous cartilage is a gold standard to repair cartilage defects. However, the application is limited due to the scarce source and secondary injury. Bone marrow-derived mesenchymal stem cells (BMSCs) are multipotent and can differentiate into cartilage in response to induction factors. Moreover, the techniques for isolating, harvesting and inducing BMSCs have become easier to use. With development of cartilage tissue engineering, scaffolds in combination with BMSCs have been frequently used to repair cartilage defects [2]. Unfortunately, ideal scaffold materials that benefit cartilage tissues are not well investigated. Studies have shown that silk fibroin (SF) and chitosan (CS) possess good bioactivity and physical properties, and have been used in tissue engineering for humans [3, 4]. However, the application of SF or CS alone exhibits some disadvantages [5, 6]. Bhardwaj et al. [7] seeded bovine chondrocytes in a SF/CS scaffold and successfully constructed tissue-engineered cartilage in vitro. Silva et al. [8] joined SF and CS together using a crosslinking agent, which can be used as a material for cartilage tissue engineering. The present study crosslinked SF and CS to construct a three-dimensional scaffold carrying BMSCs to repair cartilage defects in the rabbit knee joint.

2 Materials and methods

2.1 Design

A study of cartilage defect repair with tissue engineering techniques. This study used an animal experimental model. The procedures for animals were conducted in accordance with the Guidance Instructions for the Care and Use of Laboratory Animals, issued by the Ministry of Science and Technology of China in 2006.

2.2 Materials

New Zealand rabbits, SF/CS scaffold (prepared in-house; Fig. 1); Percoll (Gibco), Dulbecco's modified Eagle's medium (DMEM), trypsin, fetal bovine serum (FBS; HyClone); transforming growth factor-β1 (TGF-β1), dexamethasone, ascorbic acid (Sigma), scanning electron microscope (S-3400N; Hitachi, Japan) and an instron 1011 material testing machine (Chongqing University, China).

2.3 Methods

2.3.1 *Preparation of the SF/CS scaffold and evaluation of physical properties*

Preparation of SF–CS was as follows (1) extraction of SF. Natural silk was chopped, mixed with 0.5 % Na_2CO_3 and 3 g/L detergent at a mass volume ratio of 1:50 (mg:mL), degummed in a water bath at 98 ± 2 °C for 1 h, washed, and then dried at 60 °C. The degummed silk was dissolved in a solution comprising 30 % alcohol and 40 % $CaCl_2$ at a mass volume ratio of 1:70 (mg:mL) at 80 ± 2 °C, then dialyzed using a bag filter with molecular weight cutoff of 3,500 D to eliminate $CaCl_2$ and alcohol. The SF solution was stirred, condensed to 60–100 %, and centrifuged at 10,000×*g* for 30 min. SF solution was obtained after the insoluble substances were discarded. CS was completely dissolved in 1 % acetic acid solution. SF and CS were mixed at a ratio of 1:1, shaken gently, placed in a mould, and stored at −80 °C overnight. SF–CS was obtained after freeze drying using a freeze-drying machine (Freezemobile, USA). To prepare a three-dimensional SF–CS, the scaffold was placed in a mixture of 75 % methanol and 1 N NaOH for 24 h, washed, dried, placed in a crosslinking agent (50 mmol/L 1-ethyl-3-(3-dimethylaminopropyl)carbodiimide, 20 mmol/L *N*-hydroxysuccinimide) at room temperature for 8 h, then washed and dried [9].

Detection of physio-chemical properties the ultrastructure of the SF/CS complex was observed and the aperture size was measured using scanning electron microscopy. The porosity of the scaffold was determined using modified fluid displacement procedures as previously described [10]. The water absorption was also measured. Briefly, the scaffold was immersed in PBS for 24 h and dried using filter paper. The scaffold was weighed as M0, dried in a dry box for 12 h, and then weighed as M1. The water absorption of the scaffold was measured using the following formula: water absorption (%) = (M0 − M1)/M1 × 100 %. The mean value of three samples was used as the final value for water absorption.

Biomechanical detection the scaffold was prepared as cylinders of 15 × 7 mm^2, followed by tension and pressure resistance properties using an instron 1011 material testing machine at 2 mm/min. The tension test was continued until the sample was broken, and the pressure resistance test was stopped when the length of samples was reduced by 65 %. The elastic modulus and compressive strength of scaffold were determined using the following equation: (E = (F/S)/(ΔL/L) = FL/SΔL), where L is the length, S is cross-sectional area, and ΔL is the extended length in response to force (F).

2.3.2 *BMSC isolation, culture and differentiation*

Bone marrow (4 mL) was extracted from rabbit femurs using a heparinized syringe, then centrifuged and washed with PBS. The cell suspension was centrifuged with Percoll

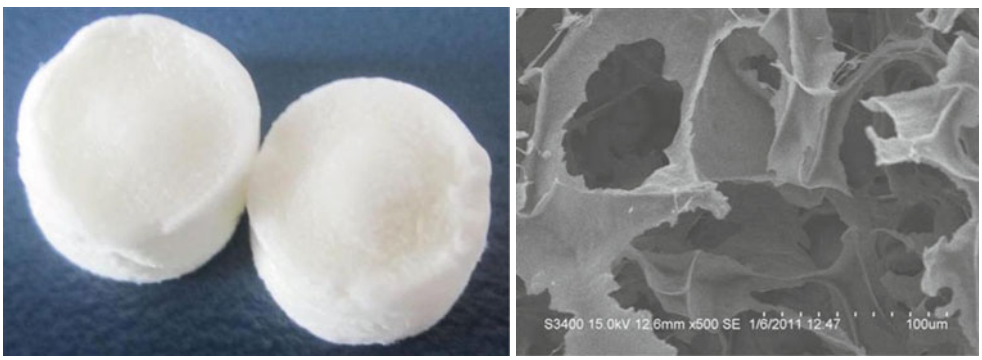

A Gross observation of the three-dimensional scaffold **B** Appearance of the scaffold under a scanning electron microscope (×500)

Fig. 1 Appearance of the silk fibroin/chitosan scaffold. **a** Gross observation of the three-dimensional scaffold; **b** Appearance of the scaffold under a scanning electron microscope (×500)

lymphocyte separation medium, and the ivory white layer in the middle was collected, PBS washed and cultured in complete low-glucose DMEM. Cells were seeded in culture flasks at 1.0×10^4 cells/cm^2 and incubated at 37 °C in a humidified atmosphere with 5 % CO_2. Half of the culture medium was exchanged after 24 h, and completely exchanged after 48 h, followed by medium changes every 2–3 days. Cells at 85 % confluency were trypsinized, centrifuged and passaged at a 1:2 ratio. Third passage cells were induced to differentiate with high-glucose DMEM containing 40 ng/mL dexamethasone, 10 ng/mL TGF-β1, 50 ng/mL ascorbic acid and 10 % FBS for 14 days. Cell differentiation was confirmed by immunohistochemical detection of type II collagen and glycosaminoglycans using toluidine blue staining.

2.3.3 Differentiation of BMSCs in the SF/CS scaffold

The adhesion of cells on SF/CS induced cells from passage three were harvested and the concentration adjusted to 1 × 105/mL. Cells were placed in cell culture plates pre-coated with SF–CS, 1 mL per well. Cells cultured in culture plates with no scaffold served as controls. Five parallel wells were used for each group. Cells were cultured in an incubator. The number of non-adhered cells was quantified at 2, 4 and 6 h. The cell adhesion rate (%) = (number of seeded cells − non-adhered cells)/number of seeded cells × 100 %.

Proliferation viability of cells on the scaffold induced cells from passage three were harvested and the concentration adjusted to 1 × 104/mL. Cells were placed in a cell culture plate pre-coated with SF–CS, 1 mL per well, and cells cultured in a culture plate with no scaffold served as controls. MTT solution, 100 μL, was added to each well at 1, 3, 5 and 7 days. Hydrochloric acid isopropyl alcohol, 1 mL, was added to each well after incubation for 4 h to dissolve blue particles completely. After shaking in a shaking table for 30 min, 150 μL of solution was harvested from each well and placed in a 96-well plate. The absorbance value was determined using an enzyme-linked immunosorbent assay reader.

Growth of cells on scaffold The SF/CS scaffold was prepared as cylinders with a 5 mm diameter and 3 mm height, ultraviolet-irradiated for 30 min on one side and then 20 min on the other side, immersed in 75 % alcohol for 30 min, washed with sterile PBS and then immersed in high-glucose DMEM for 24 h. Cell density was adjusted to 1.5×10^8 cells/mL, and cells were seeded in the SF/CS scaffold immersed in culture medium by incubation in a cell incubator for 24 h. The cell-scaffold construct was fixed in 2.5 % glutaraldehyde and then coated with gold particles. Cells on the scaffold were observed under a scanning electron microscope.

2.3.4 Preparation of the animal model and repair of cartilage defects with the cell-scaffold construct

A total of 54 rabbits, aged 2–3 months, weighing 2.5 ± 0.2 kg, of either gender, were randomly assigned to three groups ($n = 18$): BMSCs + SF/CS scaffold group, treated with the differentiated BMSCs + SF/CS scaffold; SF/CS scaffold alone group, treated with SF/CS scaffold alone; and the untreated control group. Rabbits were anesthetized with pentobarbital sodium, and the right knee joint was exposed and disinfected. A 2 cm longitudinal incision was made at the right medial patella. The femur surface of the patellofemoral joint was exposed. A round full-thickness cartilage defect with a 5 mm diameter and 3 mm depth was made at the center using an electric drill. Differentiated BMSCs + SF/CS scaffold and SF/CS scaffold alone were respectively implanted into the appropriate groups. The articular cavity was washed with normal saline, and the incision was sutured layer by layer. Penicillin (400,000 U) was intramuscularly injected over 3 days to prevent infection. Samples were harvested at 4, 8 and 12 weeks. Defects and the surrounding normal distal femur were harvested, fixed in 10 % neutral formalin for 48 h, decalcified in 15 % ethylenediamine tetraacetic acid for 3 weeks (decalcifying fluid replaced biweekly) and then embedded in paraffin, followed by gross observation, histological examination (hematoxylin–eosin, toluidine blue staining and type II collagen immunohistochemistry) and evaluation with a modified Wakitani method. Samples harvested at 12 weeks were observed under a scanning electron microscope.

2.3.5 Statistical analysis

Repaired defects were evaluated by three staff members at the Department of Pathology according to a modified Wakitani scoring system with a double-blind method. The comparison between the two-group of statistical data was performed using an independent sample t test. A value of $P < 0.05$ was considered statistically significant.

3 Results

3.1 Physical properties of the SF/CS scaffold

Scanning electron microscopy showed that the SF/CS complex was an irregular porous structure, with numerous communication pores. The mean aperture size was 155.78 μm. The porosity of the scaffold was 93.52 ± 3.68 % as determined using modified fluid displacement procedures. Thus, we determined that the water absorption of the scaffold was 143.15 ± 5.97 %; elastic modulus 28.10 ± 1.58 MPa, and the compressive strength was 0.65 ± 0.02 MPa (Fig. 2).

3.2 BMSC isolation and differentiation

The bone marrow was extracted from the bone marrow cavity, and BMSCs were isolated using density gradient centrifugation and adherence techniques. Cells were long-fusiform shaped (Fig. 3). Third passage cells were highly positive for CD29 and CD90, and weakly positive for CD45 (Fig. 4) as determined by flow cytometry. Differentiation of third passage BMSCs resulted in chondrocytes after 14 days. Dark blue particles were observed in the cytoplasm and surrounding the cells (Fig. 3), but not detected in the control group. Immunohistochemistry showed that the cells were positive for type II collagen in BMSCs + SF/CS scaffold and SF/CS scaffold alone groups (Fig. 3), but negative in the control group.

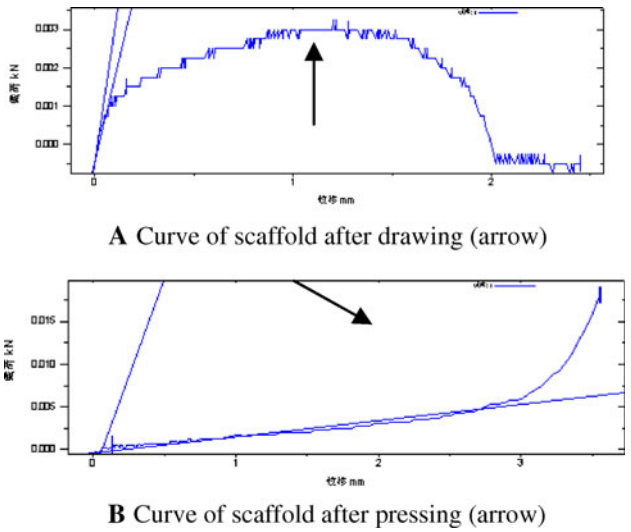

Fig. 2 Physical properties of the silk fibroin/chitosan scaffold. **a** Curve of scaffold after drawing (*arrow*); **b** Curve of scaffold after pressing (*arrow*)

3.3 Growth of differentiated BMSCs on the SF/CS scaffold

Growth of cells on scaffold at 1 day of culture, scattered round cells adhered to the scaffold and a large number of processes were observed on the cell surface. Cell microfilaments were connected with the scaffold material and a few particles were observed around the cells. At 3 days, a large number of cells had adhered to the surface and pores of the scaffold. Cells grew well and actively proliferated. Granular and filiform substances were observed around the cells. Cell microfilaments were tightly connected to the scaffold. At 5 days, an increased number of cells had adhered to the surface and pores of the scaffold compared with 3 days, and cells grew and proliferated well. Round cells became fusiform or oval-shaped (Tables 1, 2; Fig. 5).

3.4 Gross observation of repaired tissues

At 4 weeks post-surgery, defects were filled with newly generated tissues such as cartilage in the BMSCs + SF/CS scaffold group. The repair surface was not smooth, cancellated bone was not exposed and a boundary between newly generated tissues and normal cartilage was observed, which was elastic (Fig. 6a). In the SF/CS scaffold alone group, defects were filled with newly generated tissues with a dark color. The repair surface was not smooth and hollow, cancellated bone was not exposed, and a boundary between newly generated tissues and normal cartilage was observed, which was very soft (Fig. 6b). In the control group, newly generated tissues were not observed in defects (Fig. 6c). At 8 weeks post-surgery, defects remained filled with newly generated tissues such as cartilage in the BMSCs + SF/CS scaffold group. The repair surface remained smooth, and the boundary between newly generated tissues and normal cartilage was not obvious (Fig. 7a). In the SF/CS scaffold alone group, the defect surface was rough, and the boundary between newly generated tissues and normal cartilage was

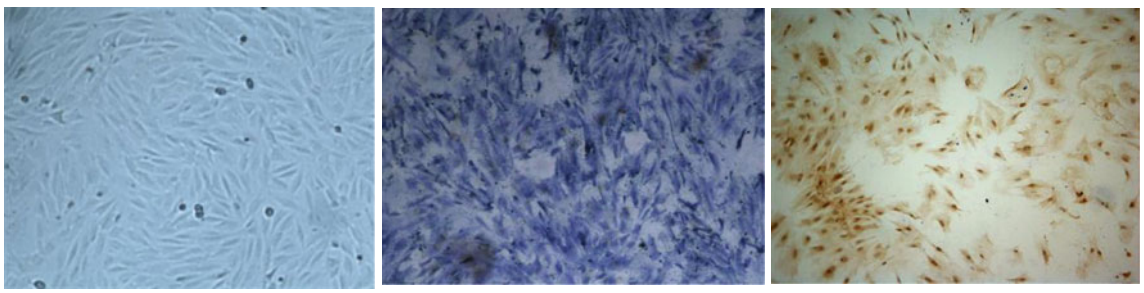

Fig. 3 **a** Third passage BMSCs; **b** Differentiated BMSCs (toluidine blue staining); **c** Differentiated BMSCs (immunohistochemical staining)

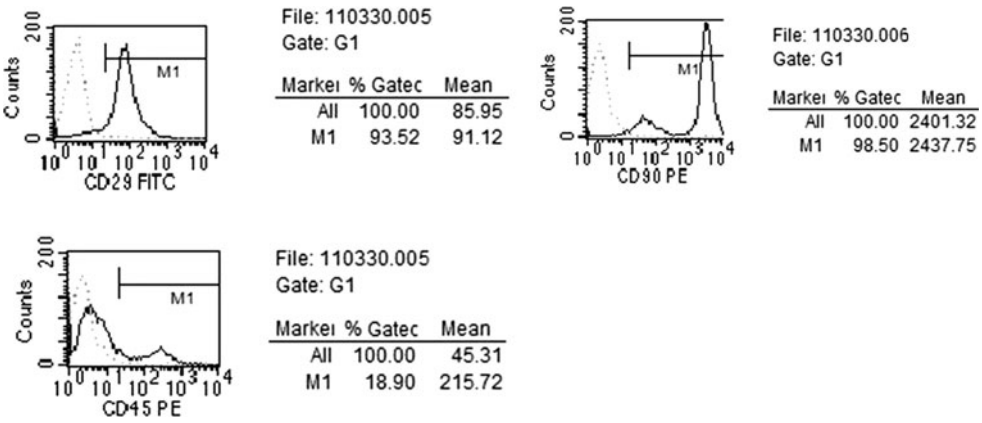

Fig. 4 Flow cytometry of third passage BMSCs shows high expression of CD29 and CD90, and low expression of CD45 (negative control)

Table 1 Adhesion rate of cells on scaffold

Group	Time (h)		
	2	4	6
Scaffold	65.44 ± 0.99	80.27 ± 1.62	88.81 ± 1.99
Control	53.05 ± 1.58▲	64.38 ± 1.78▲	77.27 ± 2.56▲

▲ $P < 0.05$, versus scaffold groups

clearly observed (Fig. 7b). In the control group, a hollow was observed in defects containing fiber-like tissues (Fig. 7c). At 12 weeks post-surgery, repaired defects exhibited a normal color with a smooth surface and elasticity, and were well connected with surrounding normal cartilage in the BMSCs + SF/CS scaffold group (Fig. 8a). In the SF/CS scaffold alone group, the defect surface was rough with a normal color and the boundary between newly generated tissues and normal cartilage was unclear, with a certain amount of elasticity (Fig. 8b). In the control group, a hollow was observed in defects containing fiber-like tissues, and the boundary between newly generated tissues and normal cartilage was clearly observed (Fig. 8c).

3.5 Histological observation

At 4 weeks post-surgery, repaired tissues were similar to normal cartilage, with fusiform-shaped cells at the surface, but the implanted cells were few and irregular, and immature chondrocytes were observed in deep layers. Cartilage lacuna and rudimental scaffold material were detected, as well as a large number of inflammatory cells in the BMSCs + SF/CS scaffold group. In the SF/CS scaffold

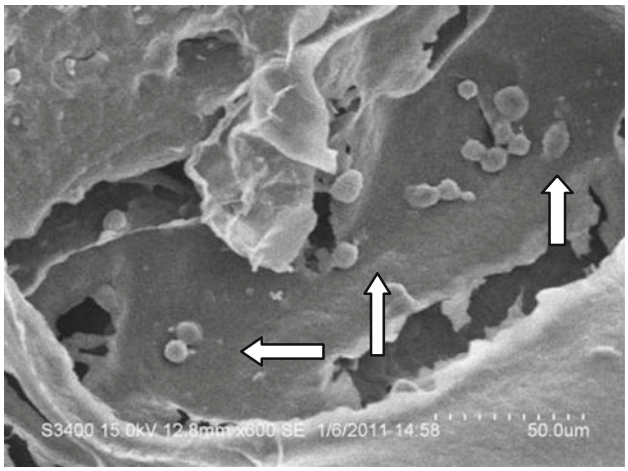

Fig. 5 BMSCs on the SF/CS scaffold (scanning electron microscope, ×600). *Arrows* cells actively proliferating

alone group, chondrocyte-like cells and lymphocytes were not observed. The scaffold was not degraded, and a large number of inflammatory cells were observed, as well as some newly generated tissues. In the control group, repaired tissues were not observed. At 8 weeks post-surgery, repaired tissues were connected to surrounding normal cartilage, with fusiform-shaped cells at the surface consisting of mainly transparent chondrocyte-like cells. Cartilage lacuna was observed, and the number of inflammatory cells was decreased in the BMSCs + SF/CS scaffold group. Some repaired tissues were observed in the SF/CS scaffold alone group, as well as degraded scaffold and inflammatory cells. In the control group, defects were filled with some fiber-like tissues. At 12 weeks post-

Table 2 Proliferation of cells on scaffold

Group	Time (day)			
	1	3	5	7
Scaffold	0.085 ± 0.041	0.244 ± 0.085	0.536 ± 0.037	0.848 ± 0.053
Control	0.063 ± 0.059*	0.170 ± 0.013*	0.381 ± 0.026*	0.658 ± 0.028*

* $P < 0.05$, versus scaffold group

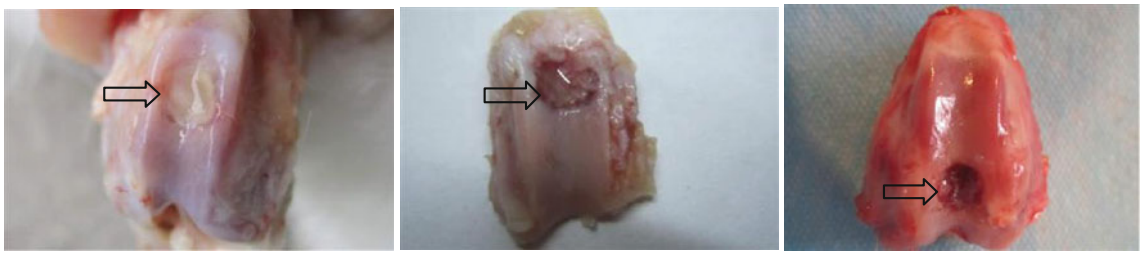

A BMSCs+SF/CS scaffold group
B SF/CS scaffold alone group
C Control group

Fig. 6 Gross observation at 4 weeks (*arrows* defects). **a** BMSCs + SF/CS scaffold group; **b** SF/CS scaffold alone group; **c** Control group

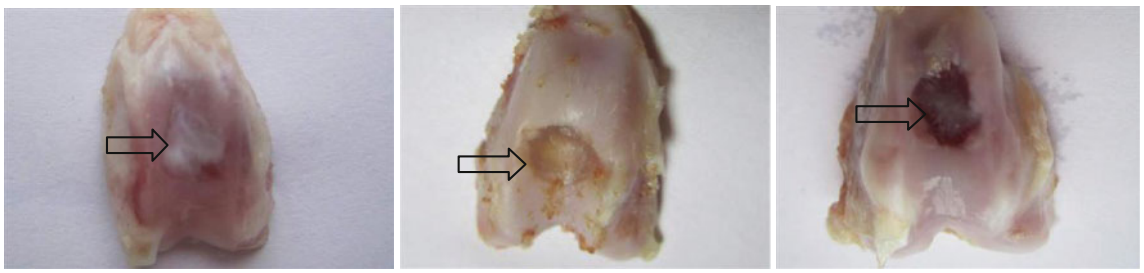

A BMSCs+SF/CS scaffold group
B SF/CS scaffold alone group
C Control group

Fig. 7 Gross observation at 8 weeks (*arrows* defects). **a** BMSCs + SF/CS scaffold group; **b** SF/CS scaffold alone group; **c** Control group

A BMSCs+SF/CS scaffold group
B SF/CS scaffold alone group
C Control group

Fig. 8 Gross observation at 12 weeks (*arrows* defects). **a** BMSCs + SF/CS scaffold group; **b** SF/CS scaffold alone group; **c** Control group

surgery, defects were repaired by transparent cartilage tissues that were nearly identical to that of normal cartilage, with mature cartilage tissues at the surface, an ordered cell arrangement and an increased number of cells. Cartilage lacuna was observed, immature chondrocytes proliferated well as colonies in deep layers in the BMSCs + SF/CS scaffold group (Fig. 9), and inflammatory cells, lymphocytes or scaffold were not observed (Figs. 10a, 11a). Immunohistochemistry showed a positive reaction for type II collagen (Fig. 12a). In the SF/CS scaffold alone group, the quantity of repaired tissues was increased, defects were repaired by fiber-like tissues that were closely connected to normal tissues. The repair thickness was thinner than that of normal cartilage. Inflammatory cells, lymphocytes or scaffold were not observed (Figs. 10b, 11b). Immunohistochemistry showed a weakly positive reaction for type II collagen (Fig. 12b). In the control group, defects were filled with fiber-like tissues (Figs. 10c, 11c), and immunohistochemistry showed a negative reaction for type II collagen (Fig. 12c).

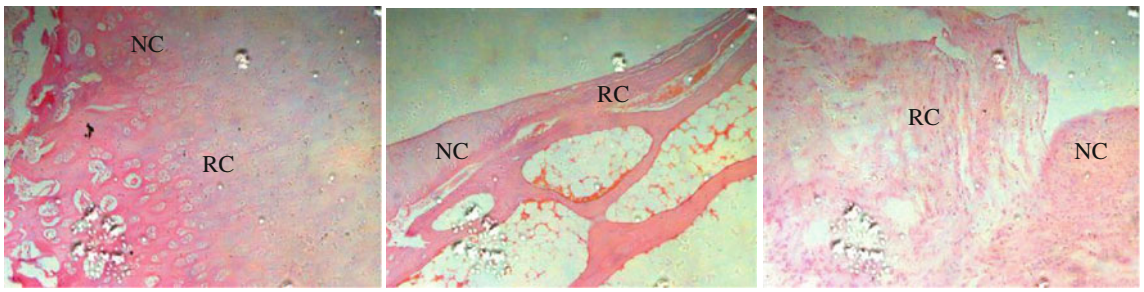

A BMSCs+SF/CS scaffold group
B SF/CS scaffold alone group
C Control group

Fig. 9 Immature chondrocytes in a deep layer of repaired tissues in the BMSCs + SF/CS scaffold group at 12 weeks (*arrows* clonal-like proliferation)

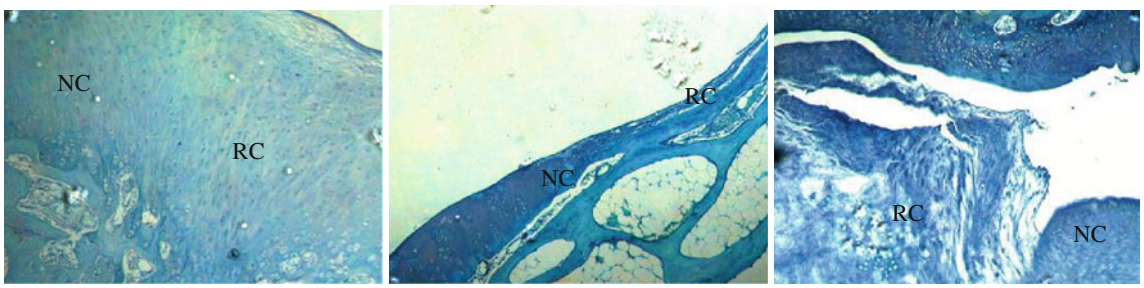

A BMSCs+SF/CS scaffold group
B SF/CS scaffold alone group
C Control group

Fig. 10 Hematoxylin–eosin staining at 12 weeks (×100). *NC* normal tissues, *RC* repaired tissues. **a** BMSCs + SF/CS scaffold group; **b** SF/CS scaffold alone group; **c** Control group

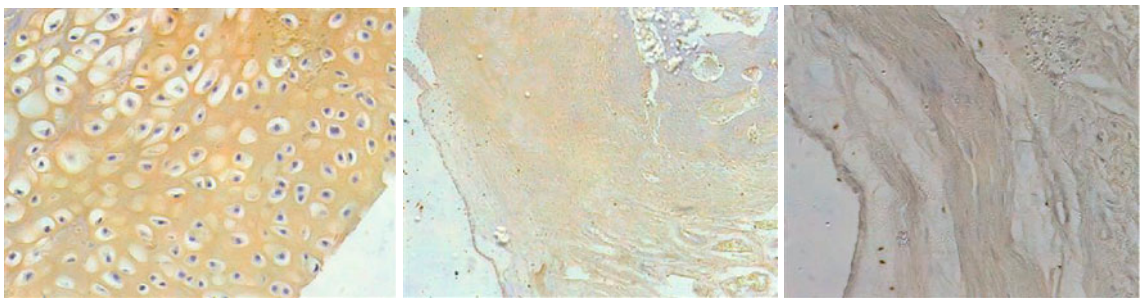

A BMSCs+SF/CS scaffold group
B SF/CS scaffold alone group
C Control group

Fig. 11 Toluidine blue staining at 12 weeks (×100). *NC* normal tissues, *RC* repaired tissues. **a** BMSCs + SF/CS scaffold group; **b** SF/CS scaffold alone group; **c** Control group

3.6 Wakitani scores [11]

Wakitani scores were significantly higher in the BMSCs + SF/CS scaffold group compared with those of the other groups at 4, 8 and 12 weeks ($P < 0.05$; Table 3).

3.7 Scanning electron microscopic observation

At 12 weeks post-surgery, a large amount of collagen fibers were observed surrounding chondrocytes in the BMSCs + SF/CS scaffold group. Scaffold material was

not detected, repaired tissues were closely connected to normal cartilage, and collagen fiber was crosslinked (Fig. 13a). In the SF/CS scaffold alone group, a large amount of fibrous tissues were observed, which were tightly connected to surrounding tissues, but no chondrocyte-like cells or scaffold material was detected (Fig. 13b). In the control group, fibrous tissues filled the defects, which were disorganized (Fig. 13c).

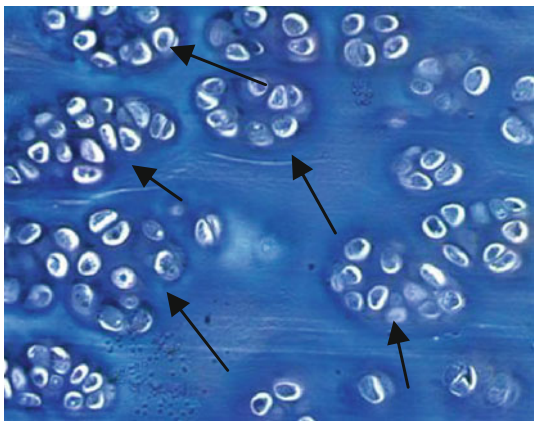

Fig. 12 Type II collagen immunohistochemistry at 12 weeks. **a** BMSCs + SF/CS scaffold group; **b** SF/CS scaffold alone group; **c** Control group

Table 3 Modified Wakitani scores at 4, 8 and 12 weeks ($n = 54$)

Group	4 weeks	8 weeks	12 weeks
BMSCs + SF/CS scaffold	8.83 ± 0.75	5.33 ± 0.82	2.33 ± 0.52
SF/CS scaffold alone	11.12 ± 1.26*	8.34 ± 0.85*	5.50 ± 0.61*
Control	11.83 ± 0.85$^{\Delta}$	10.17 ± 0.98$^{\Delta}$	7.34 ± 0.84$^{\Delta}$

* $P < 0.05$, versus BMSCs + SF/CS scaffold group; $^{\Delta}$ $P < 0.05$, versus BMSCs + F/CS scaffold group

4 Discussion

Incidence of articular cartilage injury is increased due to aging and trauma. Self-repair of cartilage is limited because of a lack of blood vessels and nerves [12]. Autologous cartilage tissues bring hope for patients with cartilage injury. A previous study showed that natural materials such as SF and CS can be used alone to serve as a scaffold, but there are some disadvantages, and autologous chondrocyte transplantation is the gold standard to repair cartilage defects [13]. However, the application is not well developed due to the limited source [14]. Therefore, it is necessary to search for an appropriate scaffold and excellent seed cells for cartilage defect repair.

4.1 Feasibility of the SF/CS scaffold as a seed cell carrier

Scaffold materials used for cartilage tissue engineering should have several properties [15, 16]. The mean aperture size should range between 100 and 300 μm to provide a sufficient three-dimensional structure for cells. Porosity should be more than 90 % to provide sufficient oxygen and nutrients. Scaffold materials should be hydrophilic to absorb nutrients and seed cells. Physical properties should resist certain pressures. Scaffold materials should possess good biocompatibility to allow cell proliferation and connection with tissues. Scaffold materials should degrade with growing tissues to not affect newly generated tissues. Scaffold materials should be cost effective, an abundant source and simple to process. SF extracted from silk and CS, deacetylated chitin, are natural polymers with good cyto- and histo-compatibility, and degrade in vivo. Gupta et al. [17] seeded endothelial cells and stem cells in a SF/CS scaffold and found that the scaffold promoted cell proliferation and migration. Altman et al. [18] seeded human adipose-derived MSCs in a SF/CS scaffold and

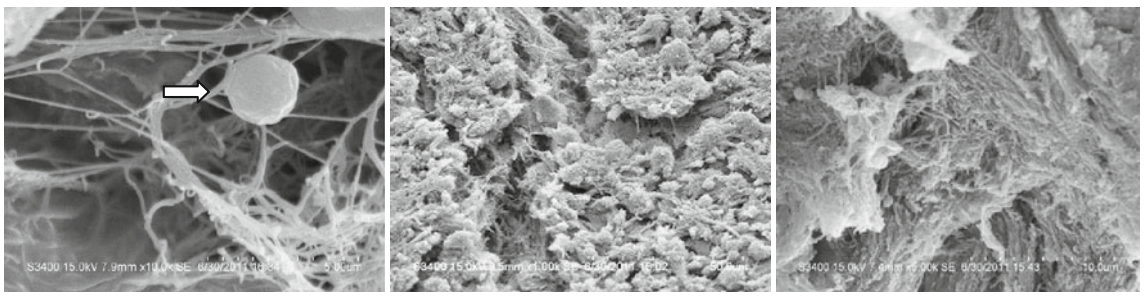

A BMSCs+SF/CS scaffold group (×10 000)

B SF/CS scaffold alone group (×5 000)

C Control group (×5 000)

Fig. 13 Observation under a scanning electron microscope. **a** BMSCs + SF/CS scaffold group (×10,000); **b** SF/CS scaffold alone group (×5,000); **c** Control group (×5,000)

found that the scaffold promoted cell attachment, migration and interaction. These results demonstrate that SF/CS scaffolds can be used as a stem cell carrier. In the present study, the SF/CS scaffold had a 155.78 μm mean aperture size, 93.52 ± 3.68 % porosity, 143.15 ± 5.97 %, water absorption expansion rate, 28.10 ± 1.58 MPa elastic modulus and 0.65 ± 0.02 MPa compressive strength. Importantly, cells actively divided on the SF/CS scaffold. The mean aperture size of the SF/CS complex was 155.78 μm. This size can provide sufficient three-dimensional structure for cell growth. A porosity of >90 % can offer sufficient oxygen and nutrition for cell growth. A high water absorption value allows the absorption of increased levels of nutrient substances to seed cells. Moreover, this scaffold can resist certain pressure and mould if necessary. It is elastic and has a three-dimensional space to prevent cell contact inhibition in surface cultures. The scaffold also has a good histocompatibility. It is cost-effective and simple to prepare. However, the rigidity of this scaffold was relatively weak.

4.2 Differentiated BMSCs combined with the SF/CS scaffold for repair of cartilage defects

Autologous chondrocytes exhibit favorable effects on clinical repair of cartilage defects. Zang et al. [19] reconstructed the trachea with a SF/CS scaffold as a chondrocyte carrier and concluded that the scaffold was beneficial for cell adherence, proliferation and differentiation, as well as enhanced accumulation of glycosaminoglycan and type II collagen. However, the quantity of chondrocytes was too small, in vitro expansion was slow and the cells may differentiate into other cell types, which leads to secondary damage to patients. BMSCs are multipotent and can differentiate into chondrocytes after induction with growth factors, and proliferate rapidly in vitro, with stable properties, low antigenicity and are an abundant cell source [20]. Therefore, BMSCs have been extensively used in tissue engineering studies. Xie et al. [21] seeded BMSCs on a polylactide-co-ε-caprolactone scaffold to repair rabbit full-thickness cartilage defects and found that the scaffold promoted the repair. In addition, bone morphogenetic protein-2-treated BMSCs have been seeded in a collagen scaffold to repair rabbit cartilage, which promoted defect repair [22]. A large number of studies demonstrate that stem cells highly express CD29 and CD90, but weakly express CD45 at the cell surface. In the present study, cells isolated from the femur using gradient centrifugation and adherence methods were identified as BMSCs. TGF-β1 is a polypeptide growth factor, which is expressed during embryogenesis, and induces BMSCs to differentiate into cartilage tissues. In the present study, third passage BMSCs were differentiated with TGF-β1 for 14 days. BMSC-derived chondrocytes have been shown to attach to SF/CS scaffolds. The SF/CS scaffold was implanted in the cartilage defect model to repair the defects under low oxygen, blood supply and synovial fluid conditions, as well as in the presence of growth factors. Defects were repaired by newly generated cartilage tissues, and repaired tissues were smooth, well connected to surrounding normal cartilage and showed high elasticity. Moreover, the SF/CS scaffold was nearly absorbed, and lymphocyte infiltration was not observed. The degradation rate of the SF/CS scaffold was consistent with tissue growth, and the immunogenicity was low. We showed that the SF/CS scaffold in combination with BMSCs can repair cartilage defects under a specific environment, which provides experimental evidence for the use of BMSCs combined with SF/CS scaffolds for the clinical treatment of articular cartilage defects. At 12 weeks, the scaffold was completely absorbed in the cartilage layer, but little remained in the subchondral bone layer. The mechanism of scaffold absorption is unknown and requires further investigation. Future studies will focus on the mechanical function and stability of newly generated tissue-engineered cartilage.

Acknowledgements Supported by the Science and Technology Program Foundation of Guizhou Province, No. [2009]2172.

References

1. Zhang HN, Li L, Leng P, Wang YZ, Lv CY. Uninduced adipose-derived stem cells repair the defect of full-thickness hyaline cartilage. Chin J Traumatol. 2009;12(2):92–7.
2. McCarty RC, Xian CJ, Gronthos S, Zannettino AC, Foster BK. Application of autologous bone marrow derived mesenchymal stem cells to an ovine model of growth plate cartilage injury. Open Orthop J. 2010;4:204–10.
3. Wang Y, Bella E, Lee CS, Migliaresi C, Pelcastre L, Schwartz Z, Boyan BD, Motta A. The synergistic effects of 3-D porous silk fibroin matrix scaffold properties and hydrodynamic environment in cartilage tissue regeneration. Biomaterials. 2010;31(17):4672–81.
4. Correia CR, Moreira-Teixeira LS, Moroni L, Reis RL, van Blitterswijk CA, Karperien M, Mano JF. Chitosan scaffolds containing hyaluronic acid for cartilage tissue engineering. Tissue Eng Part C Methods. 2011;17(7):717–30.
5. Bhumiratana S, Grayson WL, Castaneda A, Rockwood DN, Gil ES, Kaplan DL, Vunjak-Novakovic G. Nucleation and growth of mineralized bone matrix on silk-hydroxyapatite composite scaffolds. Biomaterials. 2011;32(11):2812–20.
6. Chung TW, Chang YL. Silk fibroin/chitosan-hyaluronic acid versus silk fibroin scaffolds for tissue engineering: promoting cell proliferations in vitro. Mater Sci Mater Med. 2010;21(4):1343–51.
7. Bhardwaj N, Nguyen QT, Chen AC, Kaplan DL, Sah RL, Kundu SC. Potential of 3-D tissue constructs engineered from bovine chondrocytes/silk fibroin–chitosan for in vitro cartilage tissue engineering. Biomaterials. 2011;32(25):5773–81.
8. Silva SS, Motta A, Rodrigues MT, Pinheiro AF, Gomes ME, Mano JF, Reis RL, Migliaresi C. Novel genipin-cross-linked chitosan/silk fibroin sponges for cartilage engineering strategies. Biomacromolecules. 2008;9(10):2764–74.

9. Huang WL, Deng J, Yuan SQ, et al. Investigation of silk fibroin/chitosan composite cartilage tissue-engineered scaffold. Zunyi Yixueyuan Xuebao. 2008;31(6):581–3.
10. Huang YX, Ren J, Chen C, Ren TB, Zhou XY. Preparation and properties of poly(lactide-co-glycolide) (PLGA)/nano-hydroxyapatite(NHA) scaffolds by thermally induced phase separation and rabbit MSCs culture on scaffolds. J Biomater Appl. 2008;22:409–32.
11. Wakitani S, Goto T, Young RG, Mansour JM, Goldberg VM, Caplan AI. Repair of large full-thickness articular cartilage defects with allograft articular chondrocytes embedded in a collagen gel. Tissue Eng. 1998;4(4):429–44.
12. Cosden RS, Lattermann C, Romine S, Gao J, Voss SR, MacLeod JN. Intrinsic repair of full-thickness articular cartilage defects in the axolotl salamander. Osteoarthr Cartil. 2011;19(2):200–5.
13. Guo WS, Li ZR, Cheng LM, Wang RD. The effect of subchondral bone defect in femoral head on structure and metabolism of article cartilage. Zhonghua Yi Xue Za Zhi. 2008;88(39):2795–8.
14. Yu FY, Lu SB, Zhao B, Xu WJ, Huang LH, Yuan M, Sun MX, Zhang WT. Joint resurfacing using allograft chondrocytes embedded in alginate gel. Zhonghua Yi Xue Za Zhi. 2006;86(13):886–90.
15. Chen JP, Su CH. Surface modification of electrospun PLLA nanofibers by plasma treatment and cationized gelatin immobilization for cartilage tissue engineering. Acta Biomater. 2011;7(1):234–43.
16. Shanti RM, Janjanin S, Li WJ, Nesti LJ, Mueller MB, Tzeng MB, Tuan RS. In vitro adipose tissue engineering using an electrospun nanofibrous scaffold. Ann Plast Surg. 2008;61(5):566–71.
17. Gupta V, Davis G, Gordon A, Altman AM, Reece GP, Gascoyne PR, Mathur AB. Endothelial and stem cell interactions on dielectrophoretically aligned fibrous silk fibroin–chitosan scaffolds. J Biomed Mater Res A. 2010;94(2):515–23.
18. Altman AM, Gupta V, Ríos CN, Alt EU, Mathur AB. Adhesion, migration and mechanics of human adipose-tissue-derived stem cells on silk fibroin–chitosan matrix. Acta Biomater. 2010;6(4):1388–97.
19. Zang M, Zhang Q, Davis G, Huang G, Jaffari M, Ríos CN, Gupta V, Yu P, Mathur AB. Perichondrium directed cartilage formation in silk fibroin and chitosan blend scaffolds for tracheal transplantation. Acta Biomater. 2011;7(9):3422–31.
20. Jin XH, Yang L, Duan XJ, Xie B, Li Z, Tan HB. In vivo MR imaging tracking of supermagnetic iron-oxide nanoparticle-labeled bone marrow mesenchymal stem cells injected into intra-articular space of knee joints: experiment with rabbit. Zhonghua Yi Xue Za Zhi. 2007;87(45):3213–8.
21. Xie J, Han Z, Naito M, Maeyama A, Kim SH, Kim YH, Matsuda T. Articular cartilage tissue engineering based on a mechano-active scaffold made of poly(L-lactide-co-epsilon-caprolactone): in vivo performance in adult rabbits. J Biomed Mater Res B Appl Biomater. 2010;94(1):80–8.
22. Mimura T, Imai S, Okumura N, Li L, Nishizawa K, Araki S, Ueba H, Kubo M, Mori K, Matsusue Y. Spatiotemporal control of proliferation and differentiation of bone marrow-derived mesenchymal stem cells recruited using collagen hydrogel for repair of articular cartilage defects. J Biomed Mater Res B Appl Biomater. 2011;98B(2):360–8.